Full Articles

Free electron model in cluster structure theory. Electronic structures of $[Mo_6S_8(CN)_6]^{6-}$, $[Mo_6Se_8(CN)_6]^{6-}$, $[Re_6S_8(CN)_6]^{4-}$, and $Rh_6(CO)_{16}$ clusters

V. I. Baranovski and D. V. Korol´kov★

Saint-Petersburg State University,
26 Universitetsky prosp., Peterhof, 198504 Saint-Petersburg, Russian Federation.
Fax: +7 (812) 428 6939. E-mail: koral@DK8181.spb.edu

The results of quantum chemical calculations of the electronic structure and geometry of octahedral clusters $[Mo_6S_8(CN)_6]^{6-}$, $[Mo_6Se_8(CN)_6]^{6-}$, $[Re_6S_8(CN)_6]^{4-}$, and $Rh_6(CO)_{16}$ by the *ab initio* SCF (RHF) and DFT (B3LYP) methods with various basis sets are presented. The electronic states of the clusters under study in ideal spherically symmetric potential were classified in the orbital quantum number l (1s, 1p, 1d, 1f, 1g, 1h, 1i), $l = 0—6$. In real crystal field with O_h symmetry these states are split. The calculated new electronic states were matched to the irreducible representations of the point symmetry group O_h. The polarizabilities of the compounds considered are 55—65 Å^3. A new model for the electronic structure of octahedral clusters containing M_6 groups was proposed. The model is based on the idea of free electrons moving in spherically symmetric potential field.

Key words: octahedral clusters, electronic structure, polarizability, electron density distribution, free electron "gel".

The electronic structure and bond nature in transition-metal clusters predetermine the physical and chemical properties, stability, reactivity, and the mechanisms of reactions involving these systems.[1—3] Recently, research on coordination compounds based on chalcogenide octahedral cluster complexes has been intensively developing.[4—10] Often, structural units represent clusters comprised of Re, Mo, and W atoms. These compounds are interesting by their ability to form extended linear, two-, and three-dimensional structures. Linear structures can also be formed involving transition-metals ions (Mn, Ni) coordinated to terminal ligands of the cluster. Chemical bonds in such complexes were analyzed by considering the interactions of hybridized orbitals of the metal atoms.[3,11] The energy schemes of molecular orbitals (MOs) for a number of different-type clusters of d-elements with strong- and weak-field ligands were obtained from EHT [11—13] and X_α [14] calculations. Modern quantum chemical methods permit a more detailed analysis of the nature of chemical bonds in clusters $M_nX_xY_y$.[10,15—17]

Published in Russian in *Izvestiya Akademii Nauk. Seriya Khimicheskaya,* No. 12, pp. 2617—2624, December, 2005.

1066-5285/05/5412-2705

An important characteristic of the electronic structure of the $M_nX_xY_y$ clusters comprised of heavy (4d, 5d) transition-metal atoms is the electron density distribution within the M_n core. Repeatedly calculated parameters of the electronic structure of various $M_nX_xY_y$ clusters indicate[2] effective electronic interactions between the atoms M; these are the so-called M—M cluster bonds. Sometimes, two-center M—M bonds are characterized by a rather high multiplicity (up to four). The electron density within the M_n polyhedron is always rather high along the M—M edges; it corresponds to axially symmetric M—M σ-bonds. The electron density distribution over the faces and within the M_n polyhedra of the $M_nX_xY_y$ clusters requires specific theoretical investigations. Knowledge of parameters of the electron density distribution is necessary for comparing the key characteristics of the electron-nuclear structure of transition-metal clusters $M_nX_xY_y$ with those of the cage and polyhedral hydrocarbons C_nH_m and boranes B_nH_m and a wide variety of their derivatives.

In the text below we present the results of calculations and analysis of one-electron MOs, atomic orbital (AO) populations, and electron density distribution in and polarizabilities of the octahedral clusters $[Mo_6S_8(CN)_6]^{6-}$, $[Mo_6Se_8(CN)_6]^{6-}$, $[Re_6S_8(CN)_6]^{4-}$, and $Rh_6(CO)_{16}$ with different ligands.

Calculation Procedure

Quantum chemical calculations of the electronic structure and geometry of clusters were carried out by the *ab initio* SCF method (restricted Hartree—Fock method, RHF) and density functional theory (DFT, B3LYP approximation)[18] using two basis sets (3-21G and 6-31G) for C, N, and S atoms; for Mo, Re, and Rh atoms we used the SBK effective core potentials and corresponding basis sets.[19] The molecular geometry was optimized with allowance for symmetry restrictions. It was reasonable to assume that the point symmetry group of the clusters under study is octahedral (O_h). Indeed, it was established that lowering of symmetry leads to optimized structures with somewhat higher total energies, although changes were rather small.

Often comparison of the results of geometry optimization of the clusters studied with experimental data is impossible due to the lack of the latter. The results of our calculations of the internuclear distances in the clusters $[Mo_6S_8(CN)_6]^{6-}$ (Fig. 1) and $[Mo_6Se_8(CN)_6]^{6-}$ are listed in Table 1. Experimentally determined internuclear distances in compounds $[Mo_6S_8(CN)_6]^{6-}$ and $[Mo_6S_8(py)_6]$ are respectively 2.711 and 2.644 Å for Mo—Mo and 2.573 and 2.462 Å for Mo—S.[9,20] Probably, the internuclear distances optimized in our calculations are slightly overestimated.

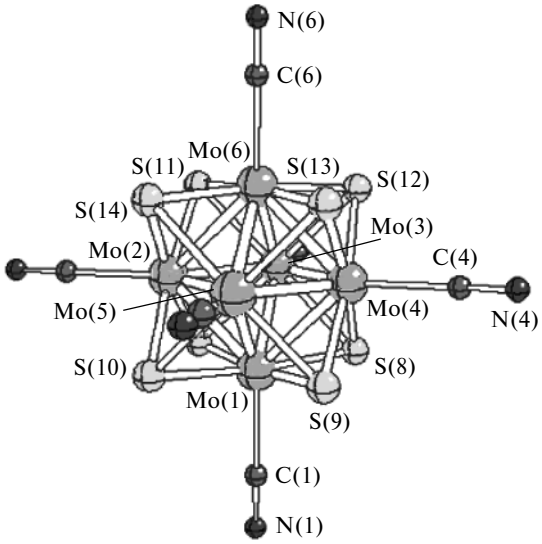

Fig. 1. Molecular structure of cluster $[Mo_6S_8(CN)_6]^{6-}$.

Calculations of the electronic structure of the clusters $[Re_6S_8(CN)_6]^{4-}$ and $Rh_6(CO)_{16}$ were carried out using experimental geometric parameters.[9,21] The bond lengths in the $[Re_6S_8(CN)_6]^{4-}$ cluster were estimated by averaging corresponding experimental data for several compounds containing the $[Re_6S_8(CN)_6]$ fragment with allowance for restrictions imposed by octahedral symmetry.

All computations including the electron density and polarizability calculations were carried out using the GAMESS program package.[22]

Results and Discussion

For all clusters studied we calculated the one-electron energies and MO compositions.

The electronic structure of the $[Mo_6S_8(CN)_6]^{6-}$ cluster includes a total of 146 occupied MOs. The lowest-

Table 1. Calculated internuclear distances (d) and effective atomic charges (q) in $[Mo_6X_8(CN)_6]^{6-}$ clusters

Method	Basis set	d/Å				q/a.u.		
		Mo—Mo	Mo—X	Mo—C	C—N	Mo	X	CN
RHF	SBK/3-21G[a]	2.7320	2.5345	2.2681	1.1610	0.239	−0.415	−0.685
	SBK/6-31G[a]	2.7351	2.5388	2.3054	1.1702	−0.127	−0.186	−0.625
B3LYP	SBK/3-21G[a]	2.7300	2.5455	2.2210	1.1845	−0.018	−0.293	−0.592
	SBK/6-31G[b]	2.8708	2.6312	2.2027	1.1960	−0.750	0.157	−0.427

[a] X = S.
[b] X = Se.

energy MOs (95 orbitals) are mainly the core AOs (Mo 3d-, 4s-, and 4p-AOs; S 1s-, 2s-, 2p-, and 3s-AOs; and N and C 1s-AOs), as well as the 1σ- and 2σ-MOs of CN groups. These MOs are symmetrized linear combinations of the AOs or MOs of CN groups. Electrons localized on these MOs can be treated, along with atomic nuclei, as a molecular skeleton, which creates a potential for the motion of other (valence) electrons that occupy the upper-lying valence MOs (a total of 51 orbital). The MO schemes obtained for the electronic structure of the same cluster from the RHF and DFT calculations obey an identical pattern. As an example, Fig. 2 shows the one-electron MO energies and MO compositions for the $[Mo_6S_8(CN)_6]^{6-}$ cluster calculated by the RHF and B3LYP methods. Here, position of each band is related to the energy of the corresponding MO; the abscissa axis shows (in relative units) the contributions of different AOs to the corresponding MO, namely, the orbitals of six Mo atoms, eight S atoms, and six CN groups; of course, the sum of these relative contributions equals unity. In discussing the results obtained it is appropriate and convenient to divide all valence MOs in the electronic structure of the clusters with respect to the type of interactions, namely: (1) Mo—S interactions and (2) interactions involving C and N atoms. In both cases the first group of valence MOs ($4t_{2u}$—$5t_{2u}$ or $9t_{2g}$—$5t_{2u}$) is almost completely composed of the Mo and S AOs. The only exception is the $13a_{1g}$ MO with a nearly 30 % contribution of the CN group orbitals. The second group of valence MOs ($11a_{1g}$—$8t_{2g}$ or $11a_{1g}$—$4t_{2u}$) has rather large contributions (up to 83%) of the AOs of CN ligands. The exceptions are the $5a_u$ and $9e_g$ MOs with zero or very small contribution of the CN component. The results obtained for nine highest occupied MOs are in good agreement with the data[16] for two clusters, $[Mo_6S_8(CN)_6]^{7-}$ and $Mo_6S_8(PH_3)_6$. The MOs of the lower-lying group can be divided[16] into MOs composed almost completely of the Mo and S AOs and MOs composed of CN group orbitals. The results of our calculations indicate a much higher degree of mixing of these orbitals. A possible reason for this distinction is the use of different computational methods in our work (SCF and DFT/B3LYP) and in the published study[16] (DV-X_α). But our results also permit discrimination of the MOs composed almost completely of the Mo and S AOs, as well as the MOs with large contributions of the CN component.

Quite similar results were obtained for the electronic structure of the $[Re_6S_8(CN)_6]^{4-}$ cluster.

In the electronic structure of the cyano clusters under study the CN group orbitals are well known σ-CN^-- and π-CN^--orbitals.

The electronic structure of the $Rh_6(CO)_{16}$ cluster includes a total of 163 occupied MOs (88 core and 75 valence MOs). The valence MOs No. 89—136 are mainly composed of the CO group orbitals with moderate contributions of the Rh AOs. A total of 27 higher-energy valence MOs (MO 137—163) are mainly composed of the metal AOs and have 10 to 35% contributions of the CO component.

NBO analysis[15] of the Mo_6S_8 fragment showed that only for the S atoms it is possible to construct the hybrid bonding orbitals mostly composed of the S3p AOs

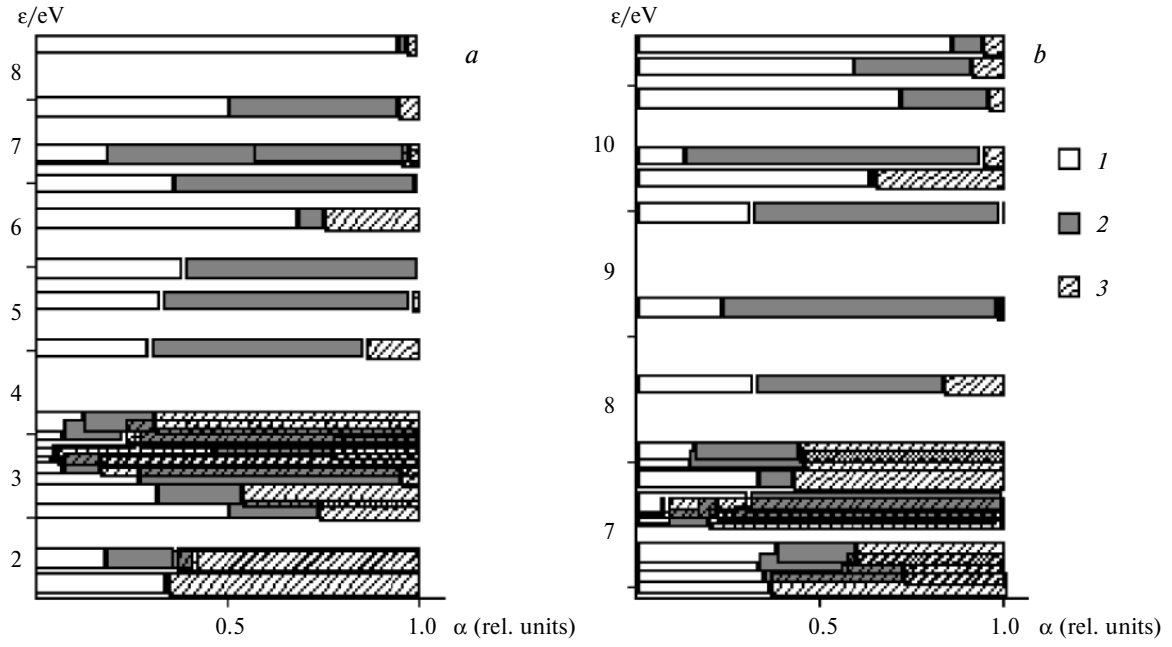

Fig. 2. MO energies and compositions of $[Mo_6S_8(CN)_6]^{6-}$ cluster obtained from RHF (*a*) and B3LYP (*b*) calculations: Mo_6 (*1*), S_8 (*2*), and $(CN^-)_6$ group (*3*); α is the AO contribution.

directed toward the Mo atoms. Deviations of these hybrid orbitals from the line connecting the Mo and S atoms reach 20—30°. The S lone electron pair orbitals are mainly (by 77%) composed of S3s AOs. For the Mo atoms, such directed bonding orbitals do not exist. There are no preferred orientations for the localized orbitals mainly composed of various linear combinations of the Mo4d AOs. Some of them are to some extent directed toward the center of the Mo_6 octahedron. Probably, mutual overlap of these orbitals in the central part of the Mo_6 octahedron can be treated as a covalent component of the bonding in the octahedral clusters under study.

Electron density distribution. The electron density distribution in the clusters in question was described using the results of calculations with the SBK/3-21G basis set. Difficulties in analysis of the electron density distribution and redistribution upon the formation of the clusters are due to the lack of information on the oxidation states of the Mo and S atoms.

For all the clusters studied we performed the population analysis. In this work, this is an auxiliary procedure; therefore, the most widely used technique was employed, namely, the Mulliken population analysis. The Mulliken atomic populations for the clusters under study are listed below.

Cluster	M	S	C	N
$[Mo_6S_8(CN)_6]^{6-}$	−0.13	−0.19	+0.08	−0.71
$[Re_6S_8(CN)_6]^{4-}$	−0.55	+0.24	+0.18	−0.61

These values are in agreement with the concepts of cluster formation from neutral metal and sulfur atoms and negatively charged CN groups involving an electron density shift from the inner "sphere" comprised of Mo atoms and from the outer "sphere" built of CN^- groups toward the intermediate "sphere" comprising sulfur atoms, namely, $Mo \rightarrow S \leftarrow CN^-$.

In the $Rh_6(CO)_{16}$ cluster, the effective charges on the equatorial and apical Rh atoms are −0.035 and +0.055, respectively.

In the electronic structure of the central fragment, Mo_6S_8, of the $[Mo_6S_8(CN)_6]^{6-}$ cluster the charge density of the electrons occupying the a_{1g} MO is mainly localized inside the Mo_6 octahedron (Fig. 3). One of the most important (in respect to spatial distribution mainly inside the Mo_6 octahedron) valence MOs, namely, the $12a_{1g}$ MO is mainly composed of the Mo s-AOs (with a large contribution of the Mo p- and d-AOs). The electron density corresponding to this MO is localized on the edges and in the interior of the Mo_6 octahedron. The next valence MO with the same symmetry, $13a_{1g}$ MO, is composed of the Mo d-AOs and corresponds to the a_{1g} MO in the electronic structure of the $[Mo_6S_8(CN)_6]^{7-}$ and $Mo_6S_8(PH_3)_6$ clusters.[16]

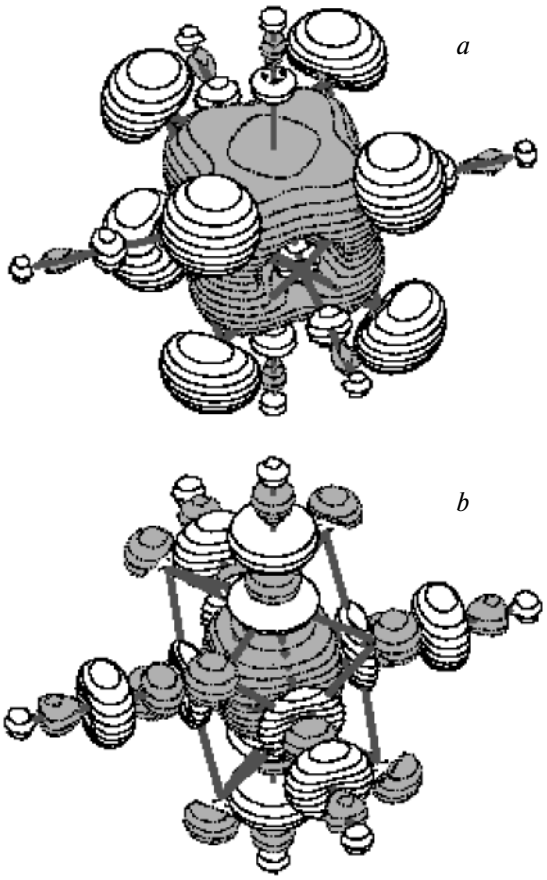

Fig. 3. Molecular orbitals $12a_{1g}$ (*a*) and $13a_{1g}$ (*b*) of cluster $[Mo_6S_8(CN)_6]^{6-}$.

We also studied the electron density distribution along the edges and over the faces and some planes of polyhedra in the $[Mo_6S_8(CN)_6]^{6-}$ and $[Re_6S_8(CN)_6]^{4-}$ clusters. The electron density along the edges of the Mo_6 polyhedron is high, being always at least 0.08 e $(a.u.)^{-3}$. There is a small but clearly seen maximum near the crossing point of the line connecting the S atom to the center of the Mo_6 polyhedron with the Mo_3 face. The electron density at the faces of the Mo_6 and Re_6 octahedra reaches a value of 0.05 e $(a.u.)^{-3}$, being also rather high in the interiors of these octahedra (0.04—0.06 e $(a.u.)^{-3}$) and uniformly distributed (Figs. 4 and 5). This region can be approximately represented by a sphere of radius 2 a.u. The effective number of electrons in this volume is $0.06(4/3)\pi R^3 \approx 2$. The electron density in the interior of the Mo_6 octahedron corresponds to the MOs with a_{1g} symmetry (see above), being to some extent due to the overlap of the molybdenum AOs.

Similar results were obtained for the $[Re_6S_8(CN)_6]^{4-}$ and $Rh_6(CO)_{16}$ clusters. For all octahedral clusters studied, the results of calculations of the electron density distribution along the edges and over the faces of the polyhedra indicate the same key features.

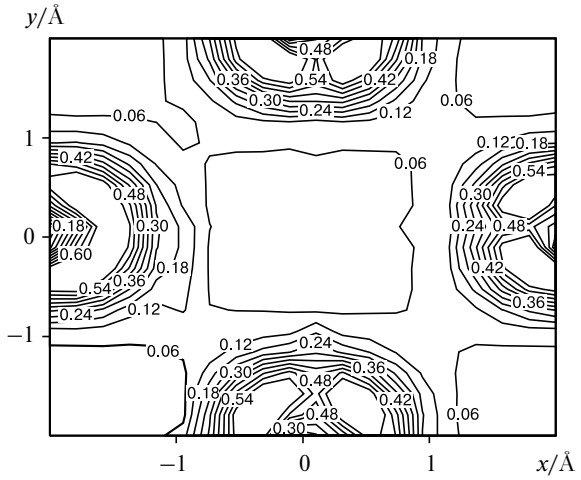

Fig. 4. The electron density distribution (in e (a.u.)$^{-3}$) in the horizontal Mo_4 plane of cluster $[Mo_6S_8(CN)_6]^{6-}$.

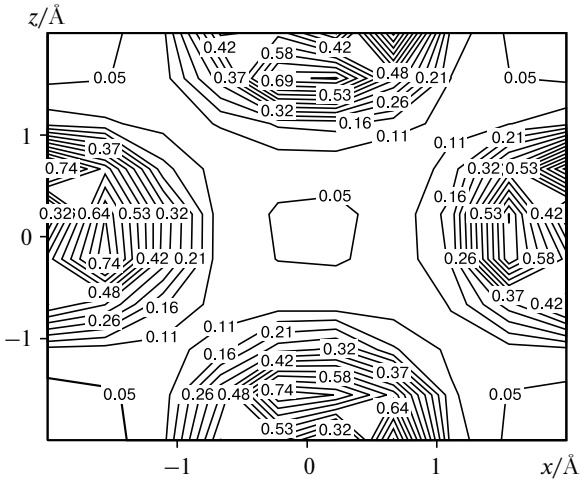

Fig. 5. The electron density distribution (in e (a.u.)$^{-3}$) in the vertical Re_4 plane of cluster $[Re_6S_8(CN)_6]^{4-}$.

Polarizabilities of octahedral clusters. Nonzero electron density inside M_6S_8 and Rh_6 octahedra suggests a high polarizability of the octahedral clusters in question. We began with polarizability studies of the Mo_6S_8 fragment. First of all, the electron density distribution in this fragment was calculated by the RHF method with different basis sets (Table 2) in order to elucidate how the basis set affects the results of polarizability calculations. It was found that the calculated polarizability of the Mo_6S_8 fragment increases by 4% only on going from the SBK/3-21G basis set (relatively small basis set without polarization and diffuse functions) to the extended basis set, SBK(f)/6-31+G*. The weak effect of the basis set on the polarizability shows that in electric field the electron density is shifted not only along the chemical bonds but also within the interior of the Mo_6 octahedron.

Table 2. Polarizability of Mo_6S_8 cluster obtained from RHF calculations with different basis sets[a]

Basis sets for Mo/S atoms	Polarizability/Å^3	
	I[b]	II[c]
3-21G/3-21G	45.5	45.6
SBK/6-31G*	46.6	46.7
SBK(f)/6-31G*	46.7	46.8
SBK(f)/6-31+G*	47.3	47.4

[a] Geometry was optimized with the SBK(f)/6-31G* basis set; d_{Mo-Mo} = 2.6157 Å, d_{Mo-S} = 2.4550 Å.
[b] Calculatied from total energy changes.
[c] Calculatied from dipole moment changes.

Table 3. Polarizabilities (α) of clusters and CN groups obtained from RHF calculations with different basis sets

Compound	α/Å^3			
	SBK/3-21G		SBK/6-31G	
	I[a]	II[b]	I[a]	II[b]
$[Mo_6S_8(CN)_6]^{6-}$	57.0	—	—	—
$[Re_6S_8(CN)_6]^{4-}$	61.9	61.8	63.6	—
$Rh_6(CO)_{16}$	51.3	51.4	53.8	53.9
CN^- [c]	2.53	2.53	3.02	3.02 (4.74)[d]
	1.04	1.04	1.23	1.23 (3.27)[d]

[a] Calculatied from total energy changes.
[b] Calculatied from dipole moment changes.
[c] Listed are the $\alpha_\parallel$ (in numerator) and $\alpha_\perp$ values (in denominator).
[d] Results of RHF/6-31+G(3d) calculations[10] are given in parentheses.

The calculated polarizabilities of all clusters under study weakly depends on the basis set (Table 3). Besides, in all cases the differences between the polarizabilities calculated from total energy changes and from dipole moment changes are negligible. The polarizability of the $[Mo_6S_8(CN)_6]^{6-}$ cluster was also estimated using the group additivity cheme

$$\alpha_\parallel([Mo_6S_8(CN)_6]^{6-}) = \alpha_\parallel(Mo_6S_8) + 2\alpha_\parallel(CN^-) + 4\alpha_\perp(CN^-)$$

using the data[23] for CN^- groups (see Table 3). The estimate obtained (~56 Å^3) is in good agreement with the results of direct calculations. This means that the CN ligands and the interior (central part) of the Mo_6S_8 fragment are polarized independently (or almost independently).

To study the electric field effect in more detail, we calculated the electron density distribution in the clusters in question in electric field applied along the M(1)—M(6) axis (Tables 4 and 5). Changes in the electron density distribution upon switching the electric field on (electric

Table 4. Effective atomic charges (q) in $[Mo_6S_8(CN)_6]^{6-}$ cluster (atomic numbering scheme is shown in Fig. 1)

Atom	q^a/a.u.		
	I[b]	II[c]	III[d]
Mo(1)	−0.127	−0.318	0.221
Mo(4)	−0.127	−0.108	−0.119
Mo(6)	−0.127	0.045	−0.138
S(7)	−0.186	−0.308	−0.417
S(11)	−0.186	−0.078	−0.040
C(1)	0.081	0.158	0.153
C(4)	0.081	0.075	0.071
C(6)	0.081	0.006	0.004
N(1)	−0.706 (−0.625)	−0.808 (−0.650)	−0.836 (−0.683)
N(4)	−0.706 (−0.625)	−0.703 (−0.628)	−0.700 (−0.629)
N(6)	−0.706 (−0.625)	−0.596 (−0.590)	−0.578 (−0.574)

[a] Effective charges on CN groups are given in parentheses.
[b] With electric field switched off.
[c] In electric field (0.01 a.u.).
[d] Optimized with electric field switched on.

Table 5. Interatomic distances (d/Å) and bond orders (W) in cluster $[Mo_6S_8(CN)_6]^{6-}$ (atomic numbering scheme is given in Fig. 1)

Atom pairs A—B	Starting structure			Optimized structure[a]	
	d_{A-B}	W_{A-B}			
		I[b]	II[c]	d_{A-B}	W_{A-B}
Mo(1)—Mo(4)	2.735	0.637	0.484	2.975	0.224
Mo(3)—Mo(4)	2.735	0.637	0.654	2.739	0.703
Mo(6)—Mo(4)	2.735	0.637	0.785	2.643	0.917
Mo(1)—S(7)	2.539	0.731	0.388	2.637	0.635
Mo(6)—S(11)	2.539	0.731	0.733	2.529	0.686
Mo(1)—C(1)	2.305	0.457	0.388	2.361	0.419
Mo(4)—C(4)	2.305	0.457	0.455	2.297	0.446
Mo(6)—C(6)	2.305	0.731	0.529	2.243	0.577
C(1)—N(1)	1.170	2.582	2.503	1.182	2.489
C(4)—N(4)	1.170	2.582	2.585	1.169	2.597
C(6)—N(6)	1.170	2.582	2.636	1.162	2.641

[a] The structure was optimized with electric field switched on.
[b] With electric field switched off.
[c] With electric field switched on.

field strength vector is directed from the lower to the upper Re atom) are shown in Fig. 6. The most important change is an antiparallel (with respect to the direction of the electric field strength vector) shift of the electron density. According to the group additivity scheme, main changes occur within the M_6 polyhedron. Additionally, there is a number of subtle but important effects that are inconsistent with the global electron density shift antiparallel to the electric field strength vector (see Fig. 6). In particular, the electron density in the outer regions of the M_6 polyhedron markedly increases near the M(6)—M_{eq} edges and decreases in the regions of the M(1)—M_{eq} bonds, being almost unchanged near the M_{eq}—M_{eq} edges. Correspondingly, the orders of the two-center bonds increase for M(6)—M_{eq}, decrease for M(1)—M_{eq}, and remain almost unhanged for M_{eq}—M_{eq} (see Table 5). These changes in the bonds orders are accompanied by antiparallel changes (a decrease, an increase, or almost constancy) in the lengths of the same bonds calculated with electric field switched on. Indeed, geometry optimization of the $[Mo_6S_8(CN)_6]^{6-}$ cluster in electric field showed that the cluster geometry changes (compared to the unperturbed starting cluster geometry) in accordance with the changes in the two-center bond orders (see Table 5). The orders of other two-center bonds also change (see Table 5).

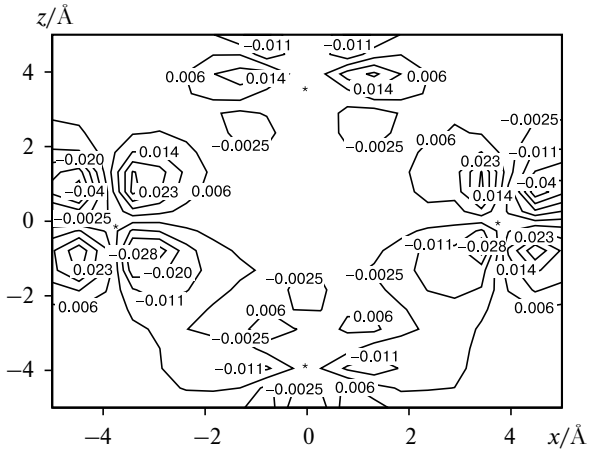

Fig. 6. Changes in electron density distribution (in e (a.u.)$^{-3}$) in vertical plane of Re_4 due to electric field effect.

Electronic structure model for octahedral clusters. Earlier,[24] a study of the electron density distribution in the cavities of adamantane $C_{10}H_{16}$ and related molecules (including ionic forms) showed that the electron density for transannular interactions on the faces of the adamantane cage, C_{10}, and within the molecular cavity is negligible compared to the electron density along C—C edges. On the contrary, in adamantane molecular cations and radical cations (adamantanyls), in particular, in the $C_{10}H_{15}^{+}$, $C_{10}H_{14}^{2+}$, $C_{10}H_{13}^{+}$, and $C_{10}H_{12}^{2+}$ fragments the electron density on certain faces and within some regions inside the C_{10} cage is comparable with the electron density on the C—C edges. This distribution is similar to electron density distribution in polyhedral boranes B_nH_m. The results obtained can be explained[24] by effective orbital interactions between the electron pairs of two-center C—C or B—B bonds and vacant quasi-atomic valence orbitals localized on transannularly arranged centers, C^+ or B.

Heavy transition metal clusters have a quite different structure. In contrast to C atoms in the adamantane and other cage or polyhedral organic molecules the M atoms

forming the inner sphere have no hybrid orbitals with appropriate shape and spatial orientation. The shape (in other words, fashion) of the electron density distribution over the cluster interiors, similar to the well-known Thomson model of atom (positively charged atomic nuclei in electron "gel") gave us an impetus to develop an improved model for the electronic structure of octahedral clusters of the 4d- and 5d-elements.

First of all it should be noted that high electron density on the faces and edges of the central octahedra M_6 corresponds to a model in which electrons are distributed over the surface of a sphere.[27] This type of electronic structure of clusters is often described using the free electron model and the tensor surface harmonics (TSH) theory. The TSH theory developed in the framework of the free electron model uses an explicit group-theory definition of the structure cluster MO.[25—27] According to this theory, the atoms M of the cluster core M_n are arranged in the surface of a sphere (*i.e.*, the centers of all atoms M are at equal distances from the center of the sphere). Each atom M is described by the angular coordinates θ_i and φ_i ($i = 1, ..., n$). Electrons of the cluster freely move across the surface of the sphere, thus simulating an idealized cluster. The electron wave functions for M_n (the number of such functions is n) are solutions to the Schrödinger equation for a particle (in our case, atom M) on a sphere; corresponding energies depend on θ_i and φ_i. Since in real clusters the atoms M form an aspherical polyhedron M_n, the orbitals and energy of a real cluster are determined from analogous characteristics of the spherical cluster using the perturbation theory with allowance for actual cluster symmetry.

The results obtained in this work (high electron density in the cluster interiors) permit extension and development of the TSH theory.

Consider four regions in the cluster:

1) inner sphere of radius 2 a.u.;

2) M_6 sphere;

3) S_8 sphere (of course, except for the rhodium carbonyl cluster); and

4) outer spherical layer comprising negatively charged CN^- groups or neutral CO groups.

As shown above, the electron density is manily localized on the core AOs and can be considered constant (fixed) inside corresponding atomic spheres. We added electrons localized on the MOs of CN^- or CO ligands to this fixed "core". All these electrons (atomic core electrons and electrons occupying ligand MOs) and atomic nuclei generate a potential in which the valence electrons move. The potential can be considered spherical; moreover, it has a nearly constant magnitude inside the cluster core M_6. This model is similar to the concept of the state of electrons within alkali-metal clusters.[28] It is known that solutions to the one-particle Schrödinger equation with spherically symmetric potential can be classified in the eigenfunctions of the $\hat{L}^2$ operator (1s, 1p, 1d, 1f, 1g, 1i). Corresponding one-electron energy levels are degenerate (degeneration multiplicity is $2l + 1$, $l = 0—6$). In the cluster field with O_h symmetry these levels are split and new one-electron states in the cluster field are transformed using the irreducible representations (IRs) of the O_h point group (Table 6). Therefore, we can determine a set of *nl* states with inclusion of splitting of the cluster field and match them to the calculated MOs. This MO scheme (after exclusion of the MOs with large contributions of CN^- groups) was constructed for both cyano clusters studied, $[Mo_6S_8(CN)_6]^{6-}$ and $[Re_6S_8(CN)_6]^{4-}$ (see Fig. 2). The proposed correlation between the calculated energy levels for octahedral molybdenum, rhenium, and rhodium clusters and the energy levels corresponding to the spherical potential model is shown in Fig. 7. It should be noted that certain IRs are unique; for instance, the a_{2u} IR is included in the f-subset only while the a_{2g} IR is included in the i-subset of states. These features of MO assignment to different *l*-subgroups illustrate the order of energies of different states of the spherical symmetry group O(3). The resulting MO scheme differs from that known for sodium clusters, namely, the MO energies increase with the orbital quantum number *l*, whereas for the Na_n clusters the 2p, 2d, *etc*. states disappear.

Table 6. Correlation between irreducible representations of spherical symmetry group O(3) and its subgroup O_h (*l* is the orbital quantum number)

l	Irreducible representations	
	Spherical symmetry group O(3)	Point symmetry group O_h
0	S	a_{1g}
1	P	t_{1u}
2	D	t_{2g}, e_g
3	F	a_{2u}, t_{1u}, t_{2u}
4	G	a_{1g}, e_g, t_{1g}, t_{2g}
5	H	e_u, $2t_{1u}$, t_{2u}
6	I	a_{1g}, a_{2g}, e_g, t_{1g}, $2t_{2g}$

In this work we put forward a model for electronic structure of octahedral clusters of 4d- and 5d-elements. Clusters are represented by sets of positively charged atomic cores "immersed' in a specific "gel" of freely moving electrons. In this case (especially taking into account the results of the electronic structure calculations for clusters in electric field, which indicate a high polarizability of the $M_nX_xY_y$ clusters) one can conclude with ease that the electron-nuclear structure of the clusters in question can be readily modified and is quite susceptible to external perturbations. Namely, changes in the internuclear

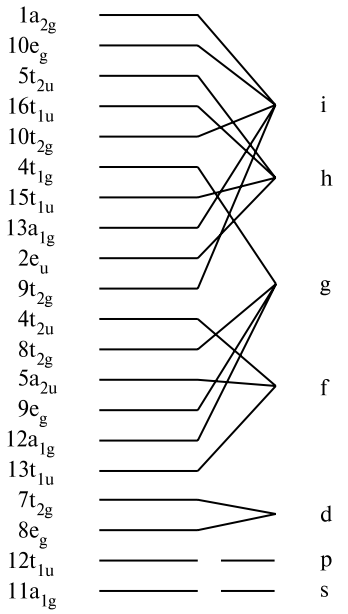

Fig. 7. Correlations between the energy levels calculated for point symmetry group O_h and proposed for spherical symmetry group O(3).

distances, changes in the spatial distribution of the valence electron density and with respect to the energy spectrum in the cluster do not require large energy expenditure and occur with ease as a response to the action of extermal factors on the cluster. Experimental data[9,21] on the addition of additional ligands or monomuclear complexes to such clusters confirm this conceptually important conclusion. Indeed, octahedral clusters of the type $[M_6X_8(CN)_6]^{q-}$ have a highly symmetric structure. But the addition of a mononuclear complex $Mn(H_2O)_5^{2+}$ or $Ni(H_2O)_5^{2+}$ to the trivalent rhenium cluster $[Re_6Se_8(CN)_6]^{4-}$ leads to distortion of the regular octahedral structure of the central polyhedron Re_6 and the differene between the Re—Re internuclear distances reaches 0.02—0.04 Å. The results of our special calculations of a modified rhodium carbonyl cluster show that replacement of a CO group in the $Rh_6(CO)_{16}$ cluster causes a marked changes (up to a few tenth of an Ångstrøm) in the geometric parameters of the cluster core.

In this work we compared the electron density distributions in three clusters, namely, $[Mo_6S_8(CN)_6]^{6-}$, $[Re_6S_8(CN)_6]^{4-}$, and $Rh_6(CO)_{16}$. The first two clusters have electron donor ligands and differ only in the number of valence electrons. The rhodium cluster has strong π-acceptors ligands. Because of this the character of the electron density distribution in the M—L space of the octahedral clusters in question is fundamentally different for the Mo and Re clusters on the one hand and the Rh cluster on the other hand. Nevertheless, the electron density distribution over the octahedral M_6 core and polarizability of all three clusters are very similar, which indicates a high strength of the M—M bonds in clusters, rather weak dependence of characteristics of these bonds on the nature of ligands and a highly conservative charactter of the bonds in the M_6 core.

Thus, we presented a convenient and quite correct model for electronic structure of octahedral clusters of heavy transition metal atoms. The model treats the clusters as sets of nuclear cores "immersed" in a "gel" of freely moving electrons, The model also seems to be applicable to clusters containing different numbers of atoms in the central fragment M_n and characterized by another symmetry of arrangement of the M atoms in the cluster space. The model proposed includes the TSH model as a limiting case corresponding to negligible electron density in the cluster interior.

All calculations were carried out at the Petrodvorets Telecommunication Center.

This work was financially supported by the INTAS (Grant 2000-00689).

References

1. D. Mingos and R. L. Johnston, *Struct. Bonding (Berlin)*, 1987, **68**, 30.
2. D. V. Korol´kov, *Koord. Khim.*, 1991, **17**, 1455 [*Sov. J. Coord. Chem.*, 1991, **17** (Engl. Transl.)].
3. Z. Lin and I. D. Williams, *Polyhedron*, 1996, **15**, 3277.
4. N. G. Naumov, A. V. Virovets, M. N. Sokolov, S. B. Artemkina, and V. E. Fedorov, *Angew. Chem., Int. Ed. Engl.*, 1998, **37**, 1943.
5. N. G. Naumov, S. B. Artemkina, A. V. Virovets, and V. E. Fedorov, *Solid. St. Sci.*, 1999, **1**, 473.
6. N. G. Naumov, S. B. Artemkina, A. V. Virovets, and V. E. Fedorov, *J. Solid. St. Chem.*, 2000, **153**, 195.
7. S. B. Artemkina, N. G. Naumov, A. V. Virovets, O. Oeckler, A. Simon, S. B. Erenburg, N. V. Bausk, and V. E. Fedorov, *Eur. J. Inorg. Chem.*, 2002, **5**, 1198.
8. S. B. Artemkina, N. G. Naumov, A. V. Virovets, S. A. Gromilov, D. Fenske, and A. V. Fedorov, *Inorg. Chem. Commun.*, 2001, **4**, 423.
9. Y. V. Mironov, A. V. Virovets, N. G. Naumov, V. N. Ikorskii, and V. E. Fedorov, *Chem. Eur. J.*, 2000, **6**, 1361.
10. S. B. Artemkina, Ph.D. (Chem.) Thesis, Inorganic Chemistry Institute, Siberian Branch of the Russian Academy of Sciences, Novosibirsk, 2003, 236 pp. (in Russian).
11. Th. G. Gray, C. M. Rudzinski, E. E. Meyer, R. H. Holm, and D. G. Nocera, *J. Am. Chem. Soc.*, 2003, **125**, 4755.
12. T. Hughbauks and R. Hoffmann, *J. Am. Chem. Soc.*, 1983, **105**, 1150.
13. R. G. Woolley, *Inorg. Chem.*, 1985, **24**, 3519.
14. L. LeBeuse, M. A. Makhyoun, R. Lissilour, and H. Chermett, *J. Chem. Phys.*, 1982, **76**, 6060.
15. A. E. Reed, L. A. Curtiss, and F. Weinhold, *Chem. Rev.*, 1988, **88**, 899.
16. H. Imoto, T. Saito, and H. Adachi, *Inorg. Chem.*, 1995, **34**, 2415.

17. V. I. Baranovski and D. V. Korolkov, *Int. J. Quant. Chem*., 2004, **100**, 343.
18. *Density Functional Theory of Atoms and Molecules*, Eds R. G. Parr and W. Yang, Oxford University Press, New York, 1988.
19. W. J. Stevens, H. Basch, M. Krauss, and P. Jasien, *Can. J. Chem*., 1992, **70**, 612.
20. S. J. Hilsenback, V. G. Young, and R. E. McCarley, *Inorg. Chem*., 1994, **33**, 1822.
21. D. H. Farrar, E. Grachova, A. Lough, Ch. Patirana, A. Poe, and S. P. Tunik, *J. Chem. Soc., Dalton Trans*., 2001, 2015.
22. M. W. Schmidt, K. K. Baldridge, J. A. Boatz, S. T. Elbert, M. S. Gordon, J. H. Jensen, S. Koseki, N. Matsunaga, K. Anguyen, S. J. Su, T. L. Windus, M. Dupuis, and J. A. Montgomery, *J. Comput. Chem*., 1993, **14**, 1347.
23. V. I. Baranovski, A. V. Kuteikina-Teplyakova, and A. I. Panin, *Zh. Strukt. Khim*., 2000, **41**, 34 [*Russ. J. Struct. Chem*., 2000, **41** (Engl. Transl.)].
24. D. V. Korolkov and O. V. Sizova, *Int. J. Quant. Chem*., 2002, **88**, 606.
25. A. J. Stone and M. Alderton, *Inorg. Chem*., 1982, **21**, 2297.
26. A. J. Stone, *Polyhedron*, 1984, **3**, 1299.
27. A. P. Klyagina, *Koord. Khim*., 1995, **21**, 612 [*Russ. J. Coord. Chem*., 1995, **21** (Engl. Transl.)].
28. W. A. de Heer, *Rev. Mod. Phys*., 1993, **65**, 611.

Received January 14, 2005;
in revised form July 15, 2005